Dual-modality PET/CT imaging: the effect of respiratory motion on combined image quality in clinical oncology

Thomas Beyer[1,2], Gerald Antoch[1], Todd Blodgett[3], Lutz F. Freudenberg[2], Tim Akhurst[4], Stephan Mueller[2]

[1] Department of Diagnostic and Interventional Radiology, University Hospital Essen, Essen, Germany
[2] Department of Nuclear Medicine, University Hospital Essen, Essen, Germany
[3] PET Facility, University of Pittsburgh Medical Center, Pittsburgh, USA
[4] Memorial Sloan Kettering Cancer Center, New York, USA

Received: 7 October 2002 / Accepted: 18 November 2002 / Published online: 12 February 2003

Abstract. To reduce potential mis-registration from differences in the breathing pattern between two complementary PET and CT data sets, patients are generally allowed to breathe quietly during a dual-modality scan using a combined PET/CT tomograph. Frequently, however, local mis-registration between the CT and the PET is observed. We have evaluated the appearance, magnitude, and frequency of respiration-induced artefacts in CT images of dual-modality PET/CT studies of 62 patients. Combined PET/CT scans during normal respiration were acquired in 43 subjects using single- or dual-slice CT. Nineteen patients were scanned with a special breathing protocol (limited breath-hold technique) on a single-slice PET/CT tomograph. All subjects were injected with ~370 MBq of FDG, and PET/CT scanning commenced 1 h post injection. The CT images were reconstructed and, after appropriate scaling, used for on-line attenuation correction of the PET emission data. We found that respiration artefacts can occur in the majority of cases if no respiration protocol is used. When applying the limited breath-hold technique, the frequency of severe artefacts in the area of the diaphragm was reduced by half, and the spatial extent of respiration-induced artefacts was reduced by at least 40% compared with the acquisition protocols without any breathing instructions. In conclusion, special breathing protocols are effective and should be used for CT scans as part of combined imaging protocols using a dual-modality PET/CT tomograph. The results of this study can also be applied to multi-slice CT to potentially reduce further breathing artefacts in PET/CT imaging and to improve overall image quality.

Thomas Beyer (✉)
Department of Diagnostic and Interventional Radiology,
University Hospital Essen, Hufelandstrasse 55,
45147 Essen, Germany
e-mail: Thomas.Beyer@uni-essen.de
Tel.: +49-201-7231528, Fax: +49-201-9597756

Keywords: PET/CT imaging – Dual-modality tomography – Oncology – Respiration protocols

Eur J Nucl Med Mol Imaging (2003) 30:588–596
DOI 10.1007/s00259-002-1097-6

Introduction

Oncologic disease is typically detected by anatomical imaging techniques, such as computed tomography (CT), which is often considered the method of choice for cancer imaging. In recent years positron emission tomography (PET), as a functional imaging technique, has gained widespread acceptance in clinical oncology for the detection of metabolic and functional abnormalities at an early stage of disease. In general, PET has a higher sensitivity and specificity than CT for the detection and staging of cancer [1]. However, the combination of PET and CT promises to be more accurate than either modality alone in the initial diagnosis and for therapy management [2].

A straightforward approach to using PET and CT together is to align the two image sets retrospectively [3]. Several computer-based algorithms have been described and research is ongoing to improve and automate these alignment techniques. So far, retrospective registration of complementary image sets works well for the brain [4], but often requires interaction with an operator to achieve an acceptable level of registration accuracy [5]. Another approach to using complementary PET and CT information is to combine the hardware into a single, dual-modality PET/CT tomograph [6].

The basic concept of combined PET/CT tomography is to examine the patient in both PET and CT mode without moving the patient off the table between examinations. Thus any potential misalignment between the two data sets is minimised, patient comfort is increased and

logistical issues with patient referral are potentially minimised [7].

In addition to providing accurately aligned functional and anatomical information, combined PET/CT offers the benefit of routine CT-based attenuation correction of the emission data [8, 9]. When using CT-based attenuation correction transmission times can be shortened to less than a minute for a whole-body scan, and transmission scans can be performed post injection without the need to correct for the bias from emission contamination.

Nevertheless, a number of issues need to be addressed in the context of complementary PET/CT imaging. Most issues pertain to the effect of methodological differences in scanning a patient with PET and CT when, at the same time, using the available CT transmission images for attenuation correction of the emission data. CT scans, for example, are typically (95%) performed in full-inspiration breath-hold with the arms up to reduce both attenuation artefacts and motion artefacts outside the heart. Current CT technology allows high-quality CT scans of the thorax or the abdomen to be completed in 20 s. In contrast, the scan time for a number of PET emission scans to cover a similar axial imaging range is in the order of several minutes. Due to the longer scan time needed, dedicated PET scans are acquired with the arms down and during normal respiration [10]. Ideally, in a combined tomograph, both CT and PET data should be acquired during the same respiratory (and cardiac) cycle. However, this is impractical in current generations of PET/CT systems, which have CT components that do not allow for efficient cardiac and respiratory gating [11] and do not routinely offer gating options for the emission acquisition. Therefore alternative solutions have to be found to best match the spatial extent of the transmission information to the average spatial distribution of the tracer activity in the emission data. This is of importance not only in matching the reconstructed anatomical and functional information but also in limiting any propagation of mis-registered CT and PET information during CT-based attenuation correction.

Goerres and colleagues showed that CT-based attenuation maps match most closely the tracer activity distribution during the emission scan when the CT is performed in end-expiration [12]. However, to ask the patient to hold his or her breath for the duration of the entire CT scan, which often extends from the lower jaw to the upper thighs, would require a very fast, multi-ring CT scanner. In addition, some cancer patients may not tolerate holding their breath in expiration or end-expiration for the duration of a whole-body CT examination. Taking into account the availability of single-slice and dual-slice CT systems and in order to minimise the stress on the patient, we suggest a limited breath-hold protocol which requires patients to hold their breath only for a limited time during the CT part of the combined PET/CT examination.

Materials and methods

Patient population. PET/CT data sets from 62 patients from three clinical sites were collected as part of this study. All patients were part of clinical protocols and had been referred for a PET/CT study by their oncology physician.

PET/CT system. The PET/CT tomograph used in this study is a BGO-based biograph (biograph BGO, Siemens Medical Solutions, Hoffman Estates, USA). The biograph BGO [11] combines a PET tomograph based on the ECAT EXACT HR+ and a Somatom Emotion CT scanner in a single, compact gantry. The CT components are available as single-slice or dual-slice CT. The transverse field of view of the CT and PET are 50 cm and 58.5 cm, respectively. The axial field of view of the PET is 15.5 cm with 63 image planes per bed position (2.4 mm slice spacing). The centres of the field of view of the CT and the PET are separated by 90 cm in the axial direction. A common patient handling system is installed at the front of the combined gantry and assures accurate positioning of patients up to 204 kg for both the CT and the PET examination.

PET/CT scanning and data processing. All patients fasted for at least 4 h prior to the PET/CT examination. An average activity of 370 MBq of fluorine-18 fluorodeoxyglucose (FDG) was injected 60 min±10 min before the examination. Patients were positioned head-first supine, and were moved to just above the first scanning position on the CT. A topogram (or scout scan) was acquired to define the axial imaging range, which for a whole-body PET/CT examination typically extended from the lower jaw to the upper thighs. A single, continuous spiral CT scan was defined on the topogram, with the total extent of the spiral being automatically matched to the closest integer number of PET bed positions. This was done to ensure sufficient CT data for CT-based attenuation correction of the PET emission data, as will be described below.

CT scan parameters were 130 kVp, 5-mm slice width, pitch 1.6, and a reconstruction increment of 2.4 mm to match the axial sampling of the reconstructed emission images. Note that the pitch was defined as the table feed per rotation divided by the nominal slice width. When necessary, the patients were given oral and/or intravenous contrast agents prior to the spiral CT scan. Depending on the axial imaging range and the number of CT detector rows, the CT transmission scan took between 40 s and 75 s. Once the CT had been completed, the table moved automatically to position the patient in the field of view of the PET. Emission scanning commenced in the caudocranial direction with the pelvis scanned first to limit artefacts in the bladder resulting from FDG excretion into the urine. Emission scan duration was 4 min to 8 min per bed position depending on the size of the patient and the preferences at each of the three sites. Typically whole-body PET/CT scans did not exceed eight bed positions (95 cm).

The CT images were reconstructed on-line and were available for CT-based attenuation correction (CT-AC) of the emission data. First the CT images were segmented into bone and non-bone using a threshold of 300 HU. The segmented images were transformed into maps of attenuation coefficients at the effective CT energy, E_{CT}. A non-bone scale factor was applied to the pixel values in the non-bone class, and a bone scale factor was applied to the pixel values in the bone class. Both scale factors were derived from the ratio of the mass attenuation coefficient of water and bone, respectively, at 511 keV and E_{CT} [8]. The presence of intravenous contrast and oral contrast agents in CT images in the context of the CT-AC described above has been discussed in [13] and [14].

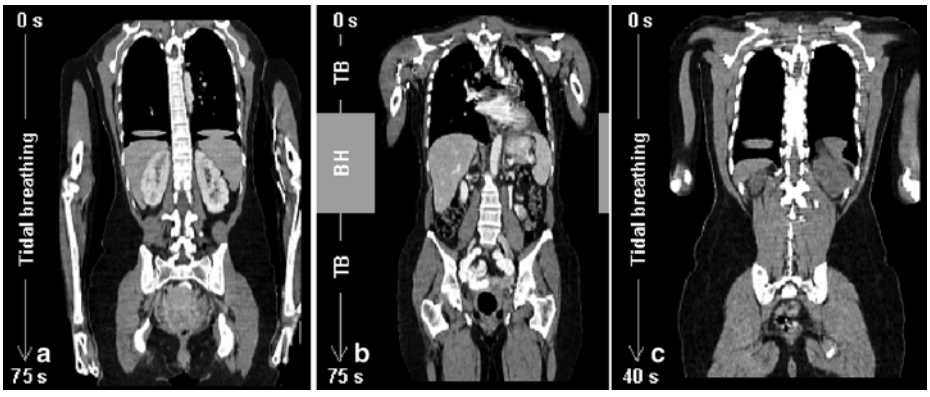

Fig. 1a–c. Three variants of CT scan acquisitions as part of the PET/CT acquisition protocols described in this study. **a** Single-slice CT during tidal breathing (TB-SS). **b** Single-slice CT and limited breath-hold (LBH-SS) technique, whereby patients were asked to hold their breath during normal respiration for as long as the spiral CT covered the lower thorax and the liver. **c** Dual-slice CT during tidal breathing (TB-DS)

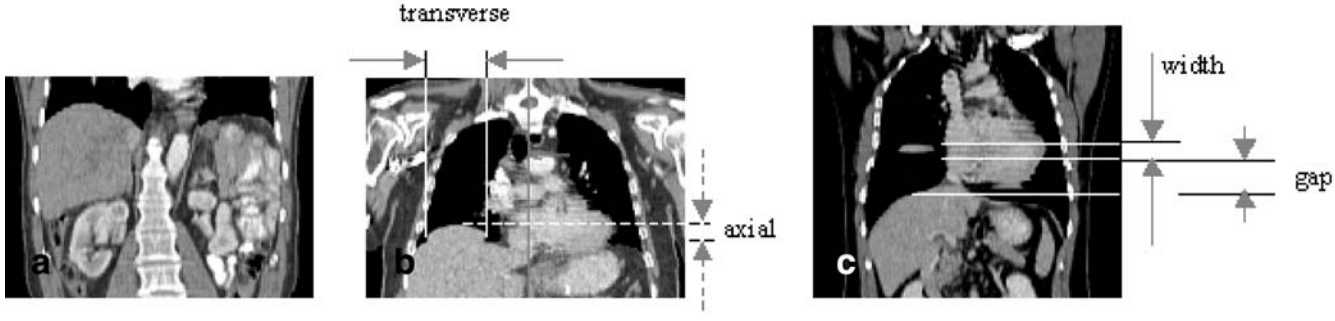

Fig. 2a–c. NMS classification scheme for CT artefacts during spiral CT scanning as part of the PET/CT imaging protocol. **a** No artefact; the surface of the liver appears smooth. **b** Mild artefacts; the liver surface appears slightly ragged and small soft tissue extensions into the lower lung can be seen. **c** Significant artefacts; artificial soft tissue densities appear detached in the mid-thorax

Table 1. Details of respiration protocols used (total no. of patients =62)

Respiration protocol	Respiration	CT	No. of patients
TB-SS	Tidal breathing	Single-slice	24
LBH-SS	Limited breath-hold	Single-slice	19
TB-DS	Tidal breathing	Dual-slice	19

Respiration protocols. All 62 patients were separated into three groups (Table 1) depending on the CT scanner and the breathing protocol: 43/62 patients were scanned on the biograph BGO with a single-slice CT, and 19/62 patients were scanned on the biograph BGO with a dual-slice CT. Of the 43 patients scanned on the single-slice CT version, 24 were instructed to breathe shallowly during the CT and the PET examination (TB-SS) while 19 were scanned with a limited breath-hold technique (LBH-SS). The 19 patients scanned on the biograph BGO with dual-slice CT were allowed to breathe shallowly during both the CT and the PET examination (TB-DS).

The respiration protocols in all three groups are illustrated in Fig. 1. The CT scan consisted of a single, continuous spiral covering an axial range from the neck to the thighs depending on the clinical indication and subsequently the number of PET bed positions. Patients following the TB-SS protocol were allowed to breathe throughout the CT scan, which took about 75 s. Patients participating in the LBH-SS protocol were asked to breathe quietly during the initial part of the CT scan starting cranially. As the field of view of the CT approached the lower mediastinum, patients were asked to expire and to hold their breath until the active field of view passed the liver (as seen on the topogram view), at which time the patients were allowed to breathe shallowly again. As with TB-SS, the total scan time for the CT was about 75 s, during which the patients held their breath for about 20 s – the time needed to cover the area of the lower mediastinum and the liver. The breathing procedure for the LBH-SS protocol was practised with the patients before the scan was started.

During the TB-DS protocol no breathing instructions were given and all subjects were scanned during tidal breathing even though the entire CT examination time could be as short as 40 s because of the faster scanning option with a dual-slice CT.

Data analysis and image evaluation. Although respiratory motion affects the thorax and the abdomen, we focussed on artefacts in the area of the diaphragm, which of all regions is affected most by respiration. For each set of PET/CT images from a single patient the whole-body CT images were evaluated for the appearance of motion artefacts between mid-thorax and mid-abdomen. Our subjective approach to the classification of the CT images (referred to here as the NMS classification) is based on three categories: *n*o artefacts, *m*ild artefacts and *s*ignificant artefacts (Fig. 2). The CT images were considered free of artefacts when the liver appeared uniform and the boundary between the liver and the lungs appeared smooth in all views (Fig. 2a). The CT images were deemed to be mildly affected by respiration if the dome of the liver extended asymmetrically into the lower lungs but these artificial soft tissue densities were still attached to the liver (Fig. 2b). If the soft tissue densities appeared completely detached from the liver and were without any morphological correlate in the mid-thorax, they were considered significant artefacts (Fig. 2c).

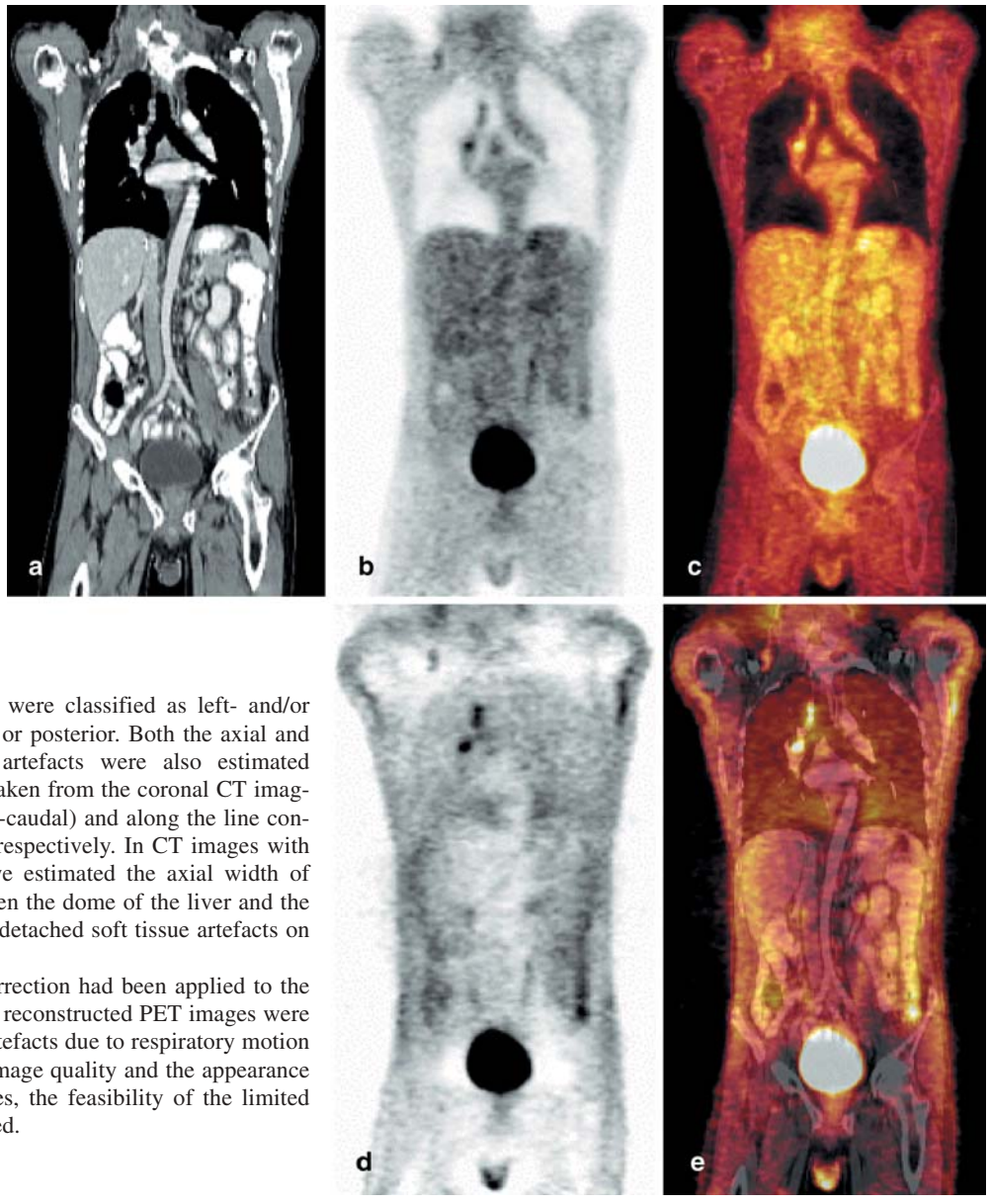

Fig. 3a–e. Example of a whole-body PET/CT study acquired with the LBH-SS protocol. The coronal CT (**a**), corrected PET (**b**) and fused PET/CT images (**c**) demonstrate the absence of respiration-induced artefacts in the vicinity of the diaphragm. For comparison, the emission data prior to attenuation correction are shown in **d** and in **e** when fused with the CT (**a**)

Mild and significant artefacts were classified as left- and/or right-sided in addition to anterior or posterior. Both the axial and the transverse extent of these artefacts were also estimated (Fig. 2b, c). Measurements were taken from the coronal CT images along the main axis (i.e. cranio-caudal) and along the line connecting the arms (i.e. left–right), respectively. In CT images with significant respiration artefacts we estimated the axial width of these artefacts, and the gap between the dome of the liver and the lower boundary of the artificially detached soft tissue artefacts on the coronal CT images (Fig. 2c).

After CT-based attenuation correction had been applied to the complementary emission data, the reconstructed PET images were evaluated for the appearance of artefacts due to respiratory motion during the CT. Based on the CT image quality and the appearance of the artefacts in the PET images, the feasibility of the limited breath-hold technique was reviewed.

Results

Figure 3 shows a PET/CT case study with no respiration artefacts in the vicinity of the diaphragm and the liver. The study was acquired using the single-slice CT and limited breath-hold (LBH-SS) protocol described above. Throughout our patient population we occasionally observed a residual discrepancy in the position of the liver on CT compared with the mean axial liver position in the emission scan, which is acquired over a large number of respiration cycles.

The number of studies with CT images free from apparent respiratory motion artefacts varied with the scan protocol. With the single-slice CT and tidal breathing (TB-SS) protocol only 1/24 studies was free of respiration artefacts, compared with 5/19 (26%) studies when applying the LBH-SS technique. Interestingly none of the patients scanned following the dual-slice CT and tidal breathing (TB-DS) protocol was free of artefacts.

Throughout our patient population, mild respiration-induced artefacts were the most frequently observed. This was true for 11/19 (58%) and 14/19 (74%) patients examined with the LBH-SS and the TB-DS protocol, respectively. An example of a patient study with mild artefacts in the right liver is shown in Fig. 4. The coronal CT image (Fig. 4a) illustrates a typical mild respiration artefact as previously described by Goerres et al. [12]. Mild artefacts were observed mostly on the patients' right side, and translated from the CT to the corrected PET images after CT-based attenuation correction. In our experience the spatial extent of these artefacts seen in the corrected PET images (Fig. 4b) was less than on the corresponding CT images.

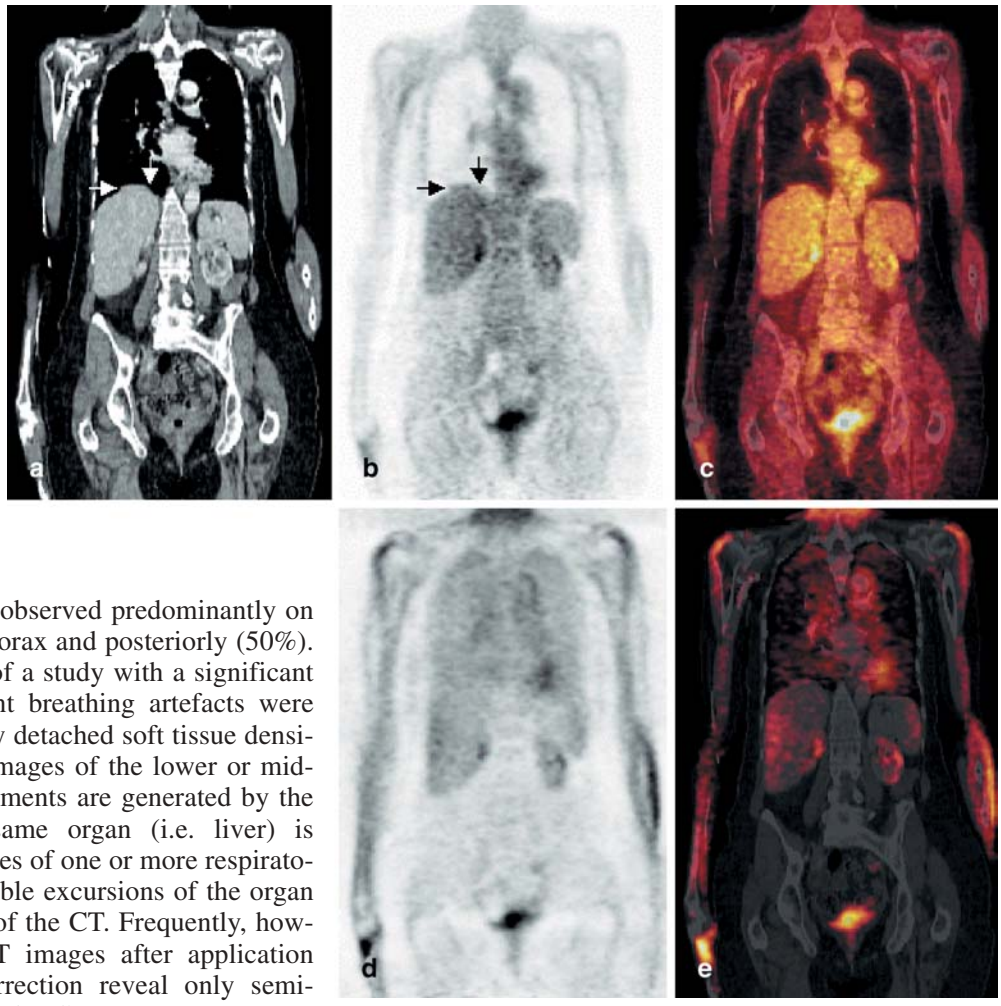

Fig. 4a–e. Mild respiration artefact seen on the coronal CT image (**a**) of a patient scanned during tidal breathing. The artefact on the PET image after CT-based attenuation correction (**b**) and on the fused image (**c**) is not as sharply delineated as on the CT image. No artefact is seen on the non-corrected emission image (**d**). Image fusion of the CT and non-corrected PET image (**e**) reveals no corresponding artefacts

Significant artefacts were observed predominantly on the right side (63%) of the thorax and posteriorly (50%). Figure 5 shows an example of a study with a significant breathing artefact. Significant breathing artefacts were considered present when fully detached soft tissue densities were visible in the CT images of the lower or mid-thorax. Such apparent detachments are generated by the CT reconstruction if the same organ (i.e. liver) is scanned during different phases of one or more respiratory cycles, which leads to visible excursions of the organ into the actual field of view of the CT. Frequently, however, the corresponding PET images after application of CT-based attenuation correction reveal only semi-detached artefacts, as seen in Fig. 5b.

Respiration artefacts were observed with varying frequencies among the three acquisition protocols. Figure 6 illustrates the frequency of mild and significant artefacts in the CT images of the 62 patients studied.

Significant artefacts occurred most frequently (16/24) when employing single-slice CT without a specific breathing protocol (TB-SS). Such artefacts were much reduced (5/19) by using a dual-slice CT system (TB-DS), and even more so by applying a limited breath-hold technique using single-slice CT (LBH-SS) (3/19). Mild artefacts were predominantly observed when using the TB-DS and LBH-SS protocols. It can be assumed that most of the significant artefacts were reduced to mild artefacts by use of the limited breath-hold technique or by use of dual-slice CT.

In all three patient groups the spatial extent of respiration-induced artefacts in the CT images varied widely. This is illustrated in Fig. 7, which compares the average axial and coronal extent of the artefacts. When applying the tidal breathing technique to single- or dual-slice CT (TB-SS or TB-DS), the average axial extent of the artefacts on CT was very similar: 21±11 mm and 22±7 mm, respectively (Fig. 7a). By using the limited breath-hold technique (LBH-SS), the axial extent was reduced to 9±8 mm on average. The average extent of mild and significant artefacts in the axial direction (Fig. 2a) is summarised in Table 2.

Table 2. Average axial extent ± standard deviation of mild and significant artefacts with all three breathing protocols. The axial extent was averaged over all patients (N), and over patients with either mild (N_m) or significant (N_s) artefacts

	Respiration protocol		
	TB-SS	LBH-SS	TB-DS
N	24	19	19
All artefacts (mm)	21±11	9±8	22±7
N_m	7	11	14
Mild artefacts (mm)	16±5	9±4	22±7
N_s	16	3	5
Significant artefacts (mm)	24±11	20±13	29±19

The coronal extent (Fig. 2b) of all respiration artefacts was also estimated (Fig. 7b). Similar to our observations on the axial extent of respiration-induced

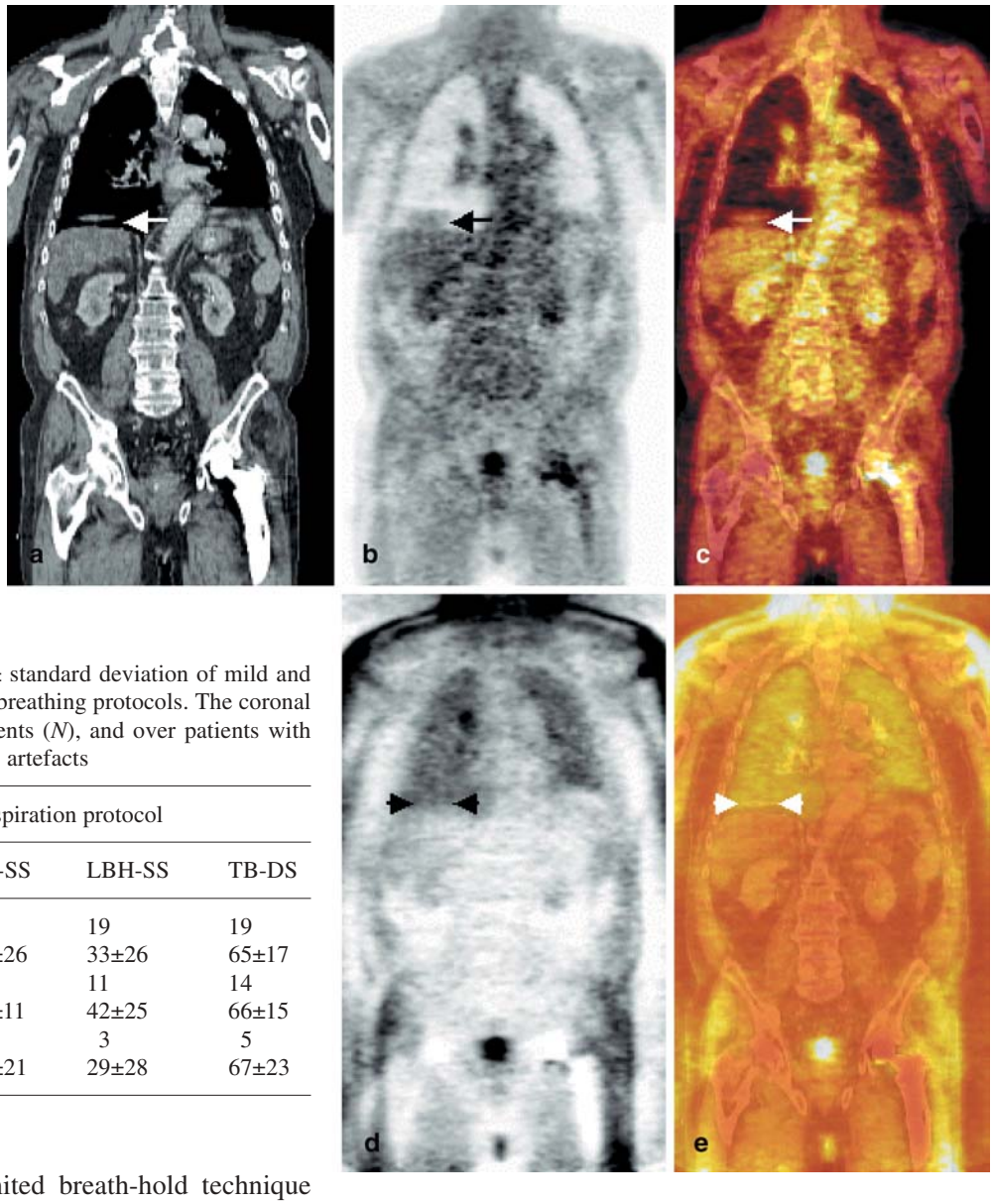

Fig. 5a–e. Example of a significant respiration artefact as seen on the coronal CT image (**a**). The corresponding corrected PET image (**b**) shows a semi-detached artefact in the region of the right liver. Image fusion of **a** and **b** in **c** illustrates the extent of the artefacts with each modality. The lung-liver boundary appears normal on the uncorrected emission (**d**) and fused emission (**e**) CT images

Table 3. Average coronal extent ± standard deviation of mild and significant artefacts with all three breathing protocols. The coronal extent was averaged over all patients (N), and over patients with either mild (N_m) or significant (N_s) artefacts

	Respiration protocol		
	TB-SS	LBH-SS	TB-DS
N	24	19	19
All artefacts (mm)	69±26	33±26	65±17
N_m	7	11	14
Mild artefacts (mm)	56±11	42±25	66±15
N_s	16	3	5
Severe artefacts (mm)	78±21	29±28	67±23

artefacts, the use of the limited breath-hold technique (LBH-SS) again reduced the extent by a factor of 2 compared with the tidal breathing technique (TB-SS and TB-DS). Differences between single-slice and dual-slice CT were small as long as no respiration protocol was used. However, with all three respiration protocols the coronal extent of the artefacts was more variable than the axial extent (compare Table 2 and Table 3).

Figure 8 illustrates the axial width of significant artefacts. Here the width refers to the distance between the upper and lower boundaries of the fully detached soft tissue

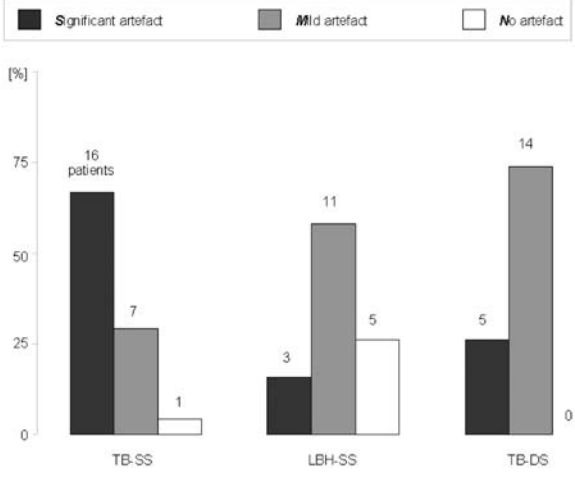

Fig. 6. Frequency (%) of respiration artefacts in 62 patients examined with dual-modality PET/CT, according to the acquisition protocols used (Table 1): TB-SS, LBH-SS or TB-DS. CT images were classified into three classes: no artefacts, mild artefacts and significant artefacts. Using a respiration protocol on a single-slice CT or using a dual-slice CT reduces the frequency of significant artefacts due to respiration on CT images

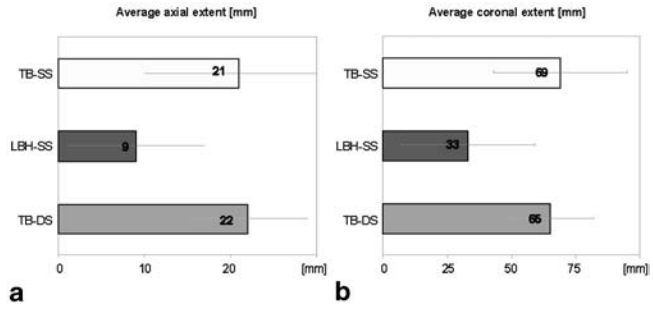

Fig. 7a, b. Average spatial extent (**a** axial, **b** coronal) of respiration artefacts in CT images of 62 patients, according to the acquisition protocol used

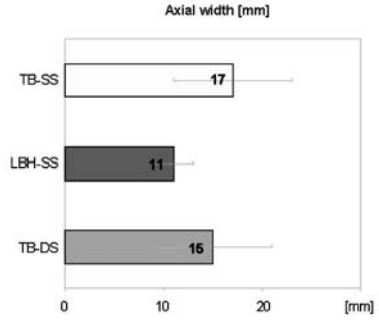

Fig. 8. Mean axial width of significant artefacts in CT images of 62 patients, according to the acquisition protocol used. The width is defined as the maximum distance between the upper and lower boundaries of fully detached soft tissue artefacts in the thorax

artefacts in the coronal CT images (Fig. 2c). If no respiration protocol was used, the maximum extent of significant artefacts was estimated to be 17±6 mm on single-slice CT (TB-SS) and 15±6 mm on dual-slice CT (TB-DS). When the limited breath-hold technique was applied to single-slice CT (LBH-SS), the width was reduced by up to 40% to 11±2 mm. The mean distance between the lower boundary of the soft tissue detachment and the diaphragm was about 13±8 mm, and ranged from as little as 4 mm to as much as 4 cm, depending on the respiration frequency.

Discussion

We found that respiration artefacts (mild and significant) occurred in 98% of all cases (42/43 patients) when no respiration technique was used (Fig. 6). The frequency of significant and mild artefacts, as well as the spatial extent of these artefacts, was reduced far more by use of the limited breath-hold technique than by use of dual-slice CT. This suggests that the introduction of a special breathing protocol is important, regardless of the number of CT detector rows available.

In the absence of respiratory gating mechanisms for routine clinical use in both CT and PET imaging, combination of CT respiration protocols and multi-slice CT seems an optimal means of reducing the frequency and magnitude of PET/CT image artefacts arising from involuntary patient motion. Nevertheless, use of the limited breath-hold technique, or any other respiration protocol, requires cooperative patients, and such a technique sometimes may be inapplicable in situations with (voluntarily or involuntarily) uncooperative patients. In our study, for example, we observed severe respiration artefacts on CT images of an extremely anxious patient, which extended up to 63 mm in the axial direction. On the other hand, the shorter scan times possible with multi-slice CT technology may help in achieving the required patient cooperation when breathing instructions are given.

Combined PET/CT image quality depends not only on the image quality of the CT and the PET but also on the processing of the available CT images for attenuation correction of the complementary emission data. To limit quantitative bias and artefacts in the corrected emission images, available transmission data need to be processed appropriately. For example, artefacts will be introduced in the corrected emission images if the spatial resolution of the transmission and the emission data is different [15]. Therefore a rebinning and filtering step is required in CT-based attenuation correction to match the spatial resolution of the CT data used for attenuation correction and the emission data. By degrading the spatial resolution of the CT by a factor of, typically, 5, large amounts of the intrinsic spatial detail information are lost. Thereby the propagation of artefacts from the CT may be reduced. This is illustrated in Fig. 9.

In our experience the appearance of mild and significant artefacts affects the image quality of PET/CT data differently. Mild respiration-induced artefacts on CT images tend to mask the reconstructed and corrected emission activity (Fig. 9a). This is the case when the CT image represents the morphology of a patient at a time in the respiratory cycle that closely matches the average tracer distribution, as measured over many respiration cycles during a PET examination. In contrast, significant respiration-induced artefacts are created by parts of the morphology captured on CT during remote excursion of the diaphragm and upper liver from their average movement during tidal respiration. If artefacts are distant from the diaphragm, they tend to create focally increased uptake patterns on the corrected emission images (Fig. 9b). If these artefacts are closer to the diaphragm, the PET activity distribution appears continuous between the liver and the apparent detachment, and no locally independent uptake patterns can be seen (Fig. 9c). In our study, artefacts were mostly observed in the vicinity of the diaphragm with 13±8 mm average distance between the upper boundary of the liver and the lower boundary of the artefact. In significant but not in mild respiration artefacts, emission activity is seen not only in the physiological variants and in the soft tis-

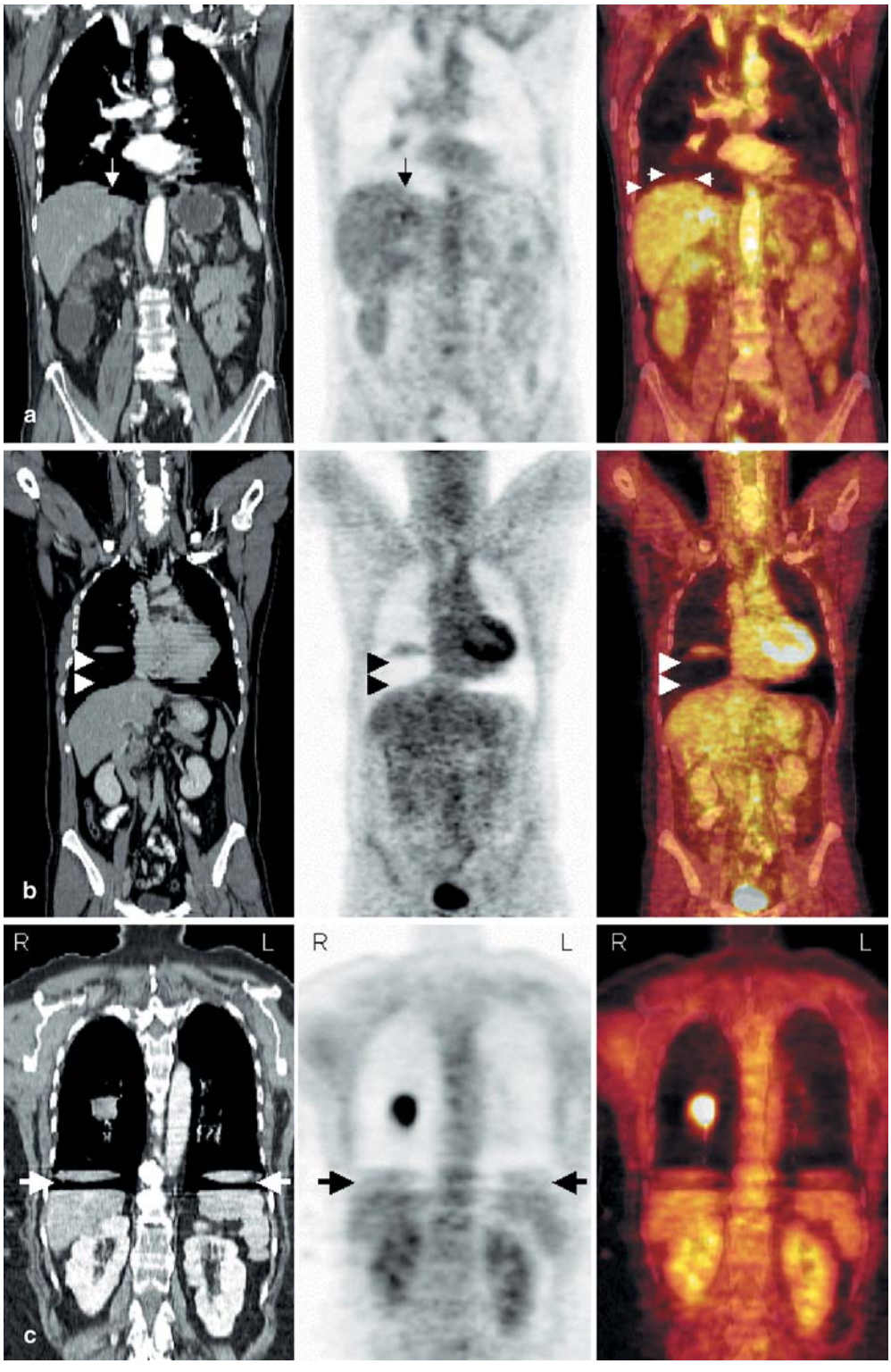

Fig. 9a–c. The appearance of mild (**a**) and significant (**b, c**) artefacts in CT and corresponding PET images after CT-based attenuation correction. Mild artefacts (*arrow* in **a**) tended to "mask" the tracer uptake pattern in the corrected PET images (**a**, *middle*). Frequently the reconstructed activity exceeded the boundary of the liver (*arrowheads* in **a**, *right*). Significant artefacts distant from the diaphragm led to the creation of separate areas of focal uptake (**b**) without intermittent tracer uptake. Artefacts closer to the diaphragm (c) did not translate into the corrected emission images accordingly, and the tracer distribution extended through the gap (*arrows*)

sue artefact but also in the space between the artefact and the normal liver (Fig. 9c). In other words, due to the periodic motion of the diaphragm during the emission scan, tracer uptake appears smeared. This may impair quantitative assessment of lesions close to the diaphragm.

As shown by other authors, respiratory motion during CT may lead to locoregional mis-registration of the CT and PET data [16, 17]. However, by viewing complementary CT and PET images acquired as part of the same dual-modality examination in fused mode, respiration-induced artefacts on CT images can be directly correlated

with artificial uptake patterns in corrected PET images (Fig. 9). Some authors recommend viewing the emission images before attenuation correction is applied in order to exclude respiration-induced bias [18]. We feel that this might be necessary in the case of lesions in the vicinity of the diaphragm. For most clinical scenarios today, however, a combined PET/CT acquisition protocol involving a carefully designed respiration technique, like the limited breath-hold protocol described here, seems sufficient.

Conclusion

In conclusion, an appropriate respiration protocol is the main determinant of artefact-free PET/CT images of the lower thorax and upper abdomen. We have shown that application of a limited breath-hold technique when acquiring the CT part of a combined PET/CT examination significantly reduces the frequency and extent of respiration-induced artefacts in the lower thorax.

Acknowledgements. The authors like to thank Paulina Khersonskaya, Sam Hsiao, Bärbel Terschüren, Sandra Pabst, and Ruth Hall for their help with the data acquisition. This paper benefited from helpful discussions with David Townsend, Jeffrey Yap, and Thomas Bruckbauer.

References

1. Gambhir SS, Czernin J, Schwimmer J, Silverman DHS, Coleman EE, Phelps ME. A tabulated summary of the FDG PET literature. J Nucl Med 2001; 42 (5 Suppl):1S–93S.
2. Vansteenkiste JF, Stroobants SG, Dupont PJ, Leyn PRD, Wever WF, Verbeken EK, Nuyts JL, Maes FP, Bogaert JG. FDG-PET scan in potentially operable non-small cell lung cancer: Do anatometabolic PET-CT fusion images improve the localisation of regional lymph node metastasis? Eur J Nucl Med 1998; 25:1495–1501.
3. Hutton BF, Braun M, Thurfjell L, Lau DYH. Image registration: an essential tool for nuclear medicine. Eur J Nucl Med 2002; 29:559–577.
4. Woods RP, Grafton ST, Holmes CJ, Cherry SR, Mazziotta JC. Automated image registration. I. General methods and intrasubject, intramodality validation. J Comput Assist Tomogr 1998; 22:139–152.
5. Yu JN, Fahey FH, Gage HD, Eades CG, Harkness BA, Pelizzari CA, Keys JW Jr. Intermodality, retrospective image registration in the thorax. J Nucl Med 1995; 36:2333–2338.
6. Townsend DW, Cherry S. Combining anatomy and function: the path to true image fusion. Eur Radiol 2001; 11:1968–1974.
7. Beyer T, Townsend DW, Brun T, Kinahan PE, Charron M, Roddy R, Jerin J, Young J, Nutt R, Byars LG. A combined PET/CT tomograph for clinical oncology. J Nucl Med 2000; 41:1369–1379.
8. Kinahan PE, Townsend DW, Beyer T, Sashin D. Attenuation correction for a combined 3D PET/CT scanner. Med Phys 1998; 25:2046–2053.
9. von Schulthess GK. Cost considerations regarding an integrated CT-PET system. Eur Radiol 2000; 10 (Suppl 3):S377–S380.
10. Hoh CK, Hawkins RA, Glaspy JA, Dahlbom M, Tse NY, Hoffman EJ, Schiepers C, Choi Y, Rege S, Nitzsche E, Maddahi J, Phelps ME. Cancer detection with whole-body PET using 2-[18F]fluoro-2-deoxy-d-glucose. J Comput Assist Tomogr 1993; 17:582–589.
11. Beyer T, Townsend D, Blodgett T. Dual-modality PET/CT tomography for clinical oncology. Q J Nucl Med 2002; 46:24–34.
12. Goerres GW, Kamel E, Heidelberg T-NH, Schwitter MR, Burger C, von Schulthess GK. PET-CT image co-registration in the thorax: influence of respiration. Eur J Nucl Med 2002; 29:351–360.
13. Beyer T, Townsend D. Dual-modality PET/CT imaging: CT-based attenuation correction in the presence of CT contrast agents. J Nucl Med 2001; 42:56P.
14. Carney J, Beyer T, Brasse D, Yap J, Townsend D. Clinical PET/CT scanning using oral CT contrast agents. J Nucl Med 2002; 43:57P.
15. Meikle SR, Dahlbom M, Cherry SR. Attenuation correction using count-limited transmission data in positron emission tomography. J Nucl Med 1993; 34:143–150.
16. Cohade C, Osman M, Wahl RL. Accuracy of PET and CT spatial registration of lung lesions with PET-CT. J Nucl Med 2002; 43:14P–15P.
17. Nakamoto Y, Cohade C, Osman M, Tatsumi M, Traughber BJ, Marshall LT, Wahl RL. Comparison of size and location of normal upper abdominal organs on PET and CT using PET/CT. J Nucl Med 2002; 43:14P.
18. Osman MM, Cohade C, Nakamoto Y, Wahl RL. Clinically significant inaccurate localization of lesions with PET-CT: frequency in 275 patients. J Nucl Med 2002; 43:32P.